# Texture Orientation of Glancing Angle Deposited Copper Nanowire Arrays

G. Mankey – University of Alabama

et al.



Citation of published version:

Alouach, H., Mankey, G. (2004): Texture Orientation of Glancing Angle Deposited Copper Nanowire Arrays. *Journal of Vacuum Science and Technology A*, 22(4).
DOI: https://doi.org/10.1116/1.1690254

# Texture orientation of glancing angle deposited copper nanowire arrays

H. Alouach and G. J. Mankey[a)]
*Center for Materials for Information Technology and Department of Physics and Astronomy, The University of Alabama, Tuscaloosa, Alabama 35487-0209*

(Received 7 October 2003; accepted 2 February 2004; published 20 July 2004)

Self-assembled copper nanowires were deposited on native oxide Si(100) substrates using glancing angle deposition with and without substrate rotation. Wire morphology, texture and crystallographic orientation are strongly dependent on the deposition parameters. A method for determining the preferred crystal orientation is described. This orientation is found to be different from what is expected from the geometric orientation of the wires. For wires deposited without substrate rotation, the face-centered-cubic (fcc)(111) crystal orientation, which corresponds to the close-packed, low surface energy (111) plane of copper, lies between the long axis of the wire and that normal to the substrate. X-ray diffraction data show that the wires exhibit bundling behavior perpendicular to the plane of incidence. For samples deposited with azimuthal rotation of the substrate, the fcc(111) directions in the wires are evenly distributed in a cone around the long axis of the wires, which point normal to the substrate. When the substrate is rotated during deposition at an angle of 75°, the wires exhibit a strong fcc(220) texture. These observations show that wires deposited with substrate rotation are highly textured and have random orientations in the plane of the substrate.  [DOI: 10.1116/1.1690254]

## I. INTRODUCTION

Self-assembled nanowire arrays have potential application in spin electronic devices such as current perpendicular to the plane (CPP) giant magnetoresistive (GMR) devices. The spin arrangements and transport properties can only be accurately estimated if the atomic-scale structure and physical properties such as wires are precisely known. Other techniques which have been developed to fabricate nanowires include electrodeposition into polymers or in insulators[1] and lithography where the pattern is transferred onto the wafer surface using high intensity ultraviolet light or a focused electron beam.[2] Recently, we have demonstrated that glancing angle deposition (GLAD) with substrate rotation can be used to produce magnetic nanowires with nanoscale dimensions.[3]

The GLAD technique[4,5] has been around for several decades, and can be used as a novel approach[6] to control three-dimensional film structure on the nanometer scale. In this process, a porous film of highly oriented nanowires is deposited by physical evaporation or sputtering with the incident beam at glancing angle. Often the film exhibits a microstructure that resembles wires with a high aspect ratio (length/width). The resulting wires are normal to the substrate or inclined depending on whether or not the substrate was rotated during deposition (Fig. 2).

Upon landing on the top of the wire, the adatoms keep part of their momentum component parallel to the substrate surface and diffuse in the direction defined by the incident beam, causing the wires to tilt from the flux incident direction toward the substrate normal. If the surface diffusion is significant, the adatoms move independently of the vapor beam direction and weaken the effect of incident momentum.[7] In general, the column inclination angle depends on the physical properties of the material and the deposition parameters. Two empirical formulas have been proposed to estimate the orientation of the long axis or the wires as a function of the deposition angle: $\tan(\beta)=1/2^{*}\tan(\alpha)$,[8] or $\beta=\alpha-\text{asin}[1/2^{*}(1-\cos(\alpha)]$,[9] where $\alpha$ is the angle between the surface normal and the incident flux and $\beta$ is the angle between the long axis of the wire and the surface normal. The crystallographic texture orientation, however, is not necessarily parallel to the direction of the wire and must be determined separately.[10]

The crystallographic texture orientation in films deposited using the GLAD technique strongly depends on the deposition parameters. Bauer applied the concept of condensation coefficient to explain observations of texture in columnar growth.[11] The condensation coefficient determines the fraction of adatoms that effectively contributes to columnar growth, and the remaining atoms fall onto the substrate and give rise to a bottom layer textured along the normal to the substrate. In the case of predominant mobility due to incident momentum, the movement of adatoms is anisotropic and aggregation of the adatoms depends on the crystallographic orientation of the crystallites. This is determined by the fast growth direction of the equilibrium crystal structure of the element that is being deposited. Crystals will tend to grow in such a way that they minimize their surface free energy. For face-centered-cubic (fcc) metals such as copper the low-energy surface is the close-packed (111) plane. In the case of columnar growth, oriented crystallites grow according to the evolutionary selection principle,[12] which takes place because of differences in the growth rates of different crystal planes, and the shadowing effect of wires that exhibit fast growth. Face-centered-cubic materials such as copper have a fast growth rate along the (110) direction, which is a large surface energy low-index plane.

[a)]Electronic mail: gmankey@mint.ua.edu

In contrast to deposition at normal flux incidence, where the substrate is the only reference plane for characterization of the film texture, in oblique incidence the plane of incidence is also a reference plane. Therefore, two crystallographic directions are needed to define the texture in oblique deposited films. In materials with a face-centered-cubic crystal structure the orientation most often found is [111](1-10), where the square brackets indicate the crystallographic direction parallel to the texture axis, and the parentheses indicate the crystallographic plane parallel to the plane of incidence.

The presence or absence of preferred orientation cannot be determined by microscopic examination.[10] The preferred orientation is solely a crystallographic condition that has nothing to do with grain shapes observed by microscopy. Only x-ray diffraction can give such evidence. In this article we present a method that allows determination of the texture orientation of nanowire arrays of samples deposited with and without substrate rotation using x-ray diffraction.

## II. EXPERIMENTAL PROCEDURE

The films were deposited in a high vacuum chamber with background pressure of less than $5\times10^{-8}$ Torr. A Telemark model 568 e-beam evaporator with integral cooling was used to deposit the films. The deposition rate was monitored by a quartz crystal microbalance placed near the substrate. Cu films were deposited onto a native oxide Si(100) substrate and the growth rate was maintained at 3 Å/s. The pressure during evaporation was $\sim5\times10^{-7}$ Torr. The vapor incidence angle measured from the normal to the substrate was 75° or 45°. The sample holder is custom designed with options for polar and azimuthal rotation. Two kinds of samples were deposited: those with and those without azimuthal rotation of the substrate.

The morphology, size, distribution and the wire inclination angle were observed using either a scanning electron microscope (Philips model XL 30) or an atomic force microscope (Digital Instruments Nanoscope IV). An x-ray diffractometer (Philips X'Pert MRD) was used for detailed structural analysis of the wires. A Cu $K\alpha$ line x-ray beam with wavelength of 1.54 Å is focused through a texture collimator on the sample and x-ray diffraction peaks are measured using a Xe gas proportional detector. The goniometer is automated and the program allows one to carry out a sequence of automated tasks for measurement and analysis.

The sample is mounted on a triple-axis sample holder and aligned by independently scanning $\Theta$ and $2\Theta$ (Fig. 1), taking the substrate silicon (400) peak as a reference. First, the goniometer is scanned in normal mode by scanning $\Theta$ and $2\Theta$ synchronously to localize angular positions of the Cu diffraction peaks. Once determined, the angular position $2\Theta$ of the Cu low energy orientation, which is perpendicular to the close-packed 111 plane, is fixed as a parameter, and the azimuthal and polar dependence of the Cu(111) peak signal is determined by scanning $\Phi$ about the normal to the specimen holder and $\Psi$ in the deposition plane about the in-plane horizontal axis, respectively.

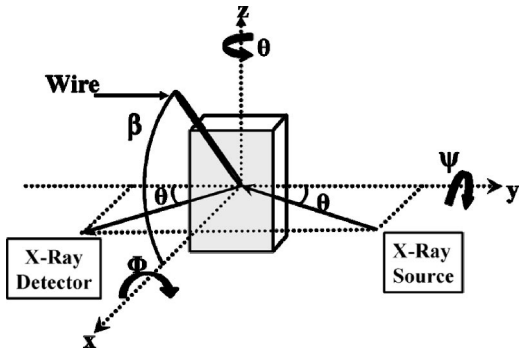


FIG. 1. Three motorized angle movements of the Philips X'Pert MRD cradle.

## III. RESULTS

The scanning electron micrographs in Fig. 2 show Cu nanowires deposited onto a native oxide Si(100) substrate at an angle of 75°. With the substrate at an angle oblique to the incident flux, areas of the substrate are shadowed by previously deposited film material that give rise to the porous structure. The inclination angle of the columns deposited without azimuthal rotation [Fig. 2(a)] is 59°, determined from cross-sectional view observations. This is near the angle (61.8°) given using the "tangent rule"

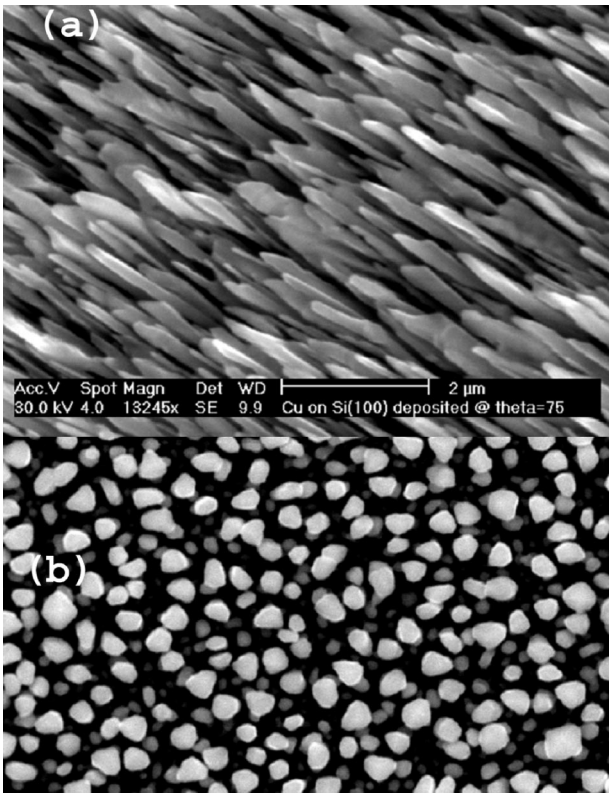


FIG. 2. Scanning electron micrographs showing highly oriented nanowire arrays of Cu deposited on native oxide Si(100) at incidence angle of 75° to the normal to the substrate. (a) Without azimuthal rotation of the substrate the wires grow inclined toward the incident beam. (b) The nanowires grow normal to the substrate when it was rotated at a rate of $3\times10^{-3}$ rotations per second.

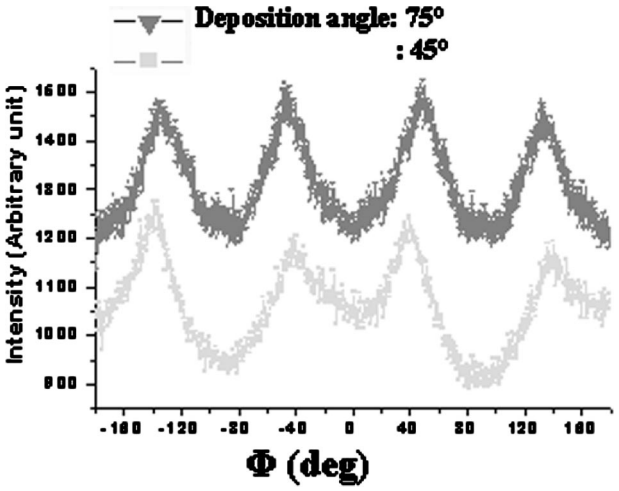


FIG. 3. Azimuthal scan of the Cu(111) peak signal of the bottom layer of the sample deposited without azimuthal rotation of the substrate. Depending on the position of the wires relative to the incident or diffracted beam, the shadow caused by the wires varies due to bundling of the wire arrays.

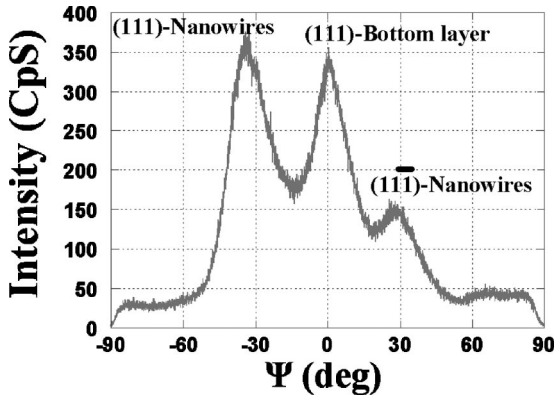


FIG. 4. Polar scans of the Cu(111) peak signal in the deposition plane. The peak at polar angle $\Psi=0$ corresponds to the Cu(111) signal of the bottom layer. The Cu(111) peak (left) indicates the texture orientation of the nanowire arrays to be 32° to the normal to the substrate. The presence of the Cu(1-11) peak (right) of the wire arrays shows that the (1-10) plane is the deposition plane for copper using GLAD.

$\tan(\beta)=1/2*\tan(\alpha)$.[8] By rotating the substrate during deposition, the columns grow normal to the plane since the shadowed regions follow rotation of the substrate [Fig. 2(b)].

As mentioned above, the GLAD film consists of two components, the wires and a continuous bottom layer that arises due to the mobility of adatoms, with two different low energy orientations. Figure 3 shows the azimuthal dependence of the Cu(111) peak signal of the GLAD film for two samples with copper deposited at different polar angles and no azimuthal rotation of the substrate. In these scans, the sample settings were optimized to investigate the bottom layer parallel to the substrate, with the deposition plane perpendicular to the sample holder at azimuthal angle $\Phi=0$. Independent of the deposition angle, the intensity is at a maximum when the wires are either facing the x-ray source or the x-ray detector; in both configurations the wires were oriented upward or downward. Due to bundling[13] of the slanted fibrous structure, the shadow caused by the wire arrays is minimal with $\Phi\sim-45°$, $+45°$, and 180° away of each of these positions, depending on the wire orientation relative to either the incident beam or the diffracted beam. Bundling of the columnar grains takes place in the direction perpendicular to the deposition plane.[14]

To look for the texture orientation angle of the wire arrays, the sample was rotated in the deposition plane. Figure 4 shows a polar scan of the Cu(111) signal of the sample deposited without substrate rotation. The peak at polar angle $\Psi=0$ corresponds to the Cu(111) signal of the bottom layer, to its left and right the Cu(111) and Cu(11-1) signals of the wire arrays, respectively. This implies that the deposition plane lies in the (1-10) crystal plane of the wires, which confirms the [111](1-10) configuration of obliquely deposited face-centered-cubic material. The angular orientation of the texture is 32° to the normal to the plane of the substrate.

The difference in intensity between the (111) and (11-1) peaks is ascribed to the defocusing effect of the x rays[15] that accompanies the rotation process and extension of the wires in the space as well. The defocusing error appears at angles more than 50° from the diffracting object (wire arrays), which is in the present case (Fig. 4) located at $\Psi=-59°$, determined by the SEM, and increases with the angular distance, causing reduction in the intensity of the peak and deformation in its shape as well.

For wires deposited with an azimuthal rotation during deposition, different behavior is observed. Figure 5 shows $2\Theta$ scans at two different polar orientations of the sample shown in Fig. 2(b). Two angular scans were performed: one along the direction of the wire normal to the substrate at $\Psi=0°$ and the other along the [111] direction at $\Psi=35.3°$. It shows that the intensity of the Cu(111) and Cu(220) signals varies in opposite ways when the sample is tilted in the polar plane while the intensity of the Cu(200) does not change. These data demonstrate that the (1-10) plane is also the deposition plane for copper deposited with azimuthal rota-

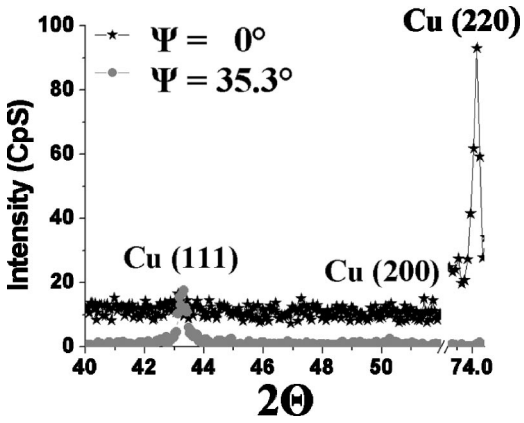


FIG. 5. $2\Theta$ x-ray scans at $\Psi=0°$ and 35.3° for the sample deposited with substrate rotation. The intensity of the Cu(111) and Cu(220) signals varies in opposite ways when the sample is tilted in the polar plane, showing that the (1-10) plane is the deposition plane. The deposition parameters were refined to give strong (220) texturing along the wire direction as shown by the $\Psi=0°$ scan.

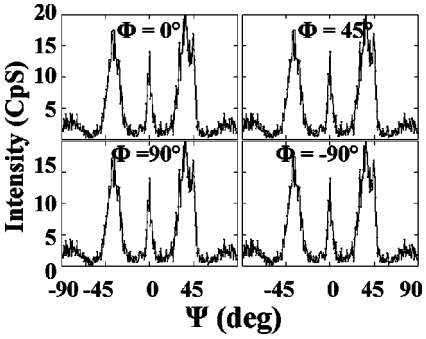


FIG. 6. Polar scan of the Cu(111) peak signal at different azimuthal orientations. Due to sample rotation during deposition the Cu(111) peak intensity is equally distributed azimuthally.

tion of the substrate. The data for $\Psi=0°$ show strong (220) texturing along the wire direction normal to the substrate.

With the wires oriented with the (110) direction normal to the substrate, the polar scans do not show any azimuthal dependence of the (111) diffraction peak (Fig. 6) since the peaks at $\Psi=0°$ (bottom layer) have the same intensity in all the scans. Due to rotation of the substrate during deposition the Cu(111) signals appear at both sides of the center peak and are equally strong for any azimuthal orientation of the wires. We conclude that the [111] crystallographic orientation is evenly distributed in a cone with a half angle of $\sim$35.3°, as illustrated in Fig. 7, whereby the [220] crystallographic direction is unique and points along the wire direction normal to the substrate.

Although the x-ray diffraction patterns in the $\Phi$ and $\Psi$ modes yield a detailed picture of the crystallographic structure of the whole sample, in the case of samples deposited with substrate rotation they give no evidence of the crystallographic orientation of each single wire separately. This raises a question as to whether the configuration depicted in Fig. 7 (left) reflects the crystallographic texture orientation of each single wire, or whether each wire actually consists of a single crystal with its Cu[220] crystal orientation along the normal to the substrate and random distribution from wire to wire of the Cu⟨111⟩ orientations throughout the whole sample. The case of Cu(111) crystal planes forming an angle

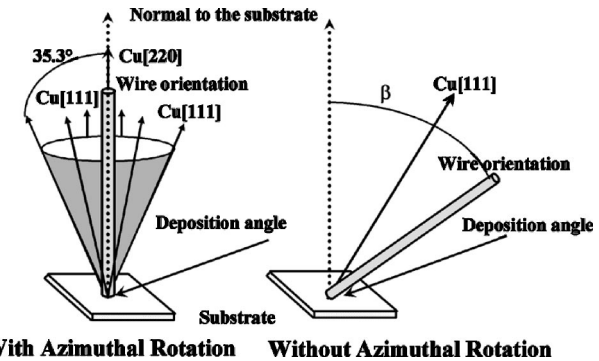


FIG. 7. Schematic diagram illustrating the effect of azimuthal rotation of the substrate during deposition on the crystallographic orientation of Cu nanowires.

of 35.3° with the substrate plane is an example of the loss of one degree of freedom, as reported by Bauer.[11] The Sherrer formula[15] for extracting grain size from the width of the diffraction peak yields a grain size of about 30 nm for wires that are microns in length. Since other factors such as the crystal mosaic that originates from a distribution of wire orientations may contribute to the linewidth, this evidence suggests that individual wires consist of only a few grains or are single crystals.

## IV. CONCLUSION

Using x-ray diffraction, we have successfully demonstrated on copper films a [111](1-10) configuration of face-centered-cubic materials and the bundling property of nanowire arrays deposited using glancing angle deposition. For samples deposited without azimuthal rotation, the texture lies between the wire direction and the normal to the substrate as a result of the momentum effect. For samples deposited with azimuthal rotation of the substrate, the [111] low energy orientation of copper is evenly distributed in a cone around the wire's geometrical orientation normal to the substrate. At a deposition angle of 75°, the sample exhibits strong (220) texturing along the wire direction. The self-assembly process may be further refined to produce individual wires for use in applications such as CPP-GMR sensors. The performance of these sensors depends on details of the structure of the interfaces so precise determination of the wire crystallography is required.

## ACKNOWLEDGMENTS

This work was funded by grants, Grant No. NSF ECS-0331864 and shared equipment Grant No. NSF-DMR-021 3985.

[1]L. Piraux, J. M. Geoarge, J. F. Despres, C. Leroy, E. Ferain, and R. Legras, Appl. Phys. Lett. **65**, 2484 (1994).
[2]P. Vavassori, G. Zangari, C. T. Yu, H. Jiang, and G. J. Mankey, J. Appl. Phys. **91**, 7992 (2002).
[3]F. Liu, C. Yu, L. Shen, J. Barnard, and G. J. Mankey, IEEE Trans. Magn. **36**, 2939 (2000).
[4]K. Robbie and M. J. Brett, J. Vac. Sci. Technol. A **15**, 1460 (1997).
[5]B. Dick, M. J. Brett, T. J. Smy, M. R. Freeman, M. Malac, and M. F. Egerton, J. Vac. Sci. Technol. A **18**, 1838 (2000).
[6]Y. P. Zhao, D. X. Ye, G. C. Wang, and T. M. Lu, Nano Lett. **2**, 351 (2002).
[7]K. Hara, J. Sci. Hiroshima Univ., Ser. A-2 **34**, 139 (1970); **34**, 163 (1970).
[8]J. M. Nieuwenhuizen and H. B. Haanstra, Philips Tech. Rev. **27**, 87 (1966).
[9]R. N. Tait, T. Smy, and M. J. Brett, Thin Solid Films **226**, 196 (1993).
[10]T. Hashimoto, K. Okamoto, K. Hara, M. Kamiya, and H. Fujiwara, Thin Solid Films **91**, 145 (1982).
[11]E. Bauer, *Single-Crystal Films*, Proceedings of an International Conference held at Philco Scientific Laboratory, Blue Bell, PA, edited by M. H. Francombe and H. Sato (Pergamon, Oxford, 1964), pp. 43; 65.
[12]A. Van der Drift, Philips Res. Rep. **22**, 267 (1967).
[13]D. O. Smith, M. S. Cohen, and G. P. Weiss, J. Appl. Phys. **31**, 1755 (1960).
[14]H. J. Leamy and A. G. Dirks, J. Phys. D **10**, L95 (1977).
[15]B. D. Cullity, *Elements of X-Ray Diffraction*, 2nd ed. (Addison–Wesley, Reading, MA, 1978).